AD-783 607

EXTENDED ARRAY EVALUATION PROGRAM.
SPECIAL REPORT NO. 15.   EVALUATION OF AN
ADAPTIVE THREE-COMPONENT FILTER

Stephen S. Lane

Texas Instruments, Incorporated

Prepared for:

Advanced Research Projects Agency
Air Force Technical Applications Center

30 November 1973

AD 783 607

REPORT DOCUMENTATION PAGE		READ INSTRUCTIONS BEFORE COMPLETING FORM
1. REPORT NUMBER	2. GOVT ACCESSION NO.	3. RECIPIENT'S CATALOG NUMBER
4. TITLE (and Subtitle) EVALUATION OF AN ADAPTIVE THREE-COMPONENT FILTER		5. TYPE OF REPORT & PERIOD COVERED Special
		6. PERFORMING ORG. REPORT NUMBER ALEX(01)-STR-73-15
7. AUTHOR(s) Stephen S. Lane		8. CONTRACT OR GRANT NUMBER(s) F33657-72-C-0725
9. PERFORMING ORGANIZATION NAME AND ADDRESS Texas Instruments Incorporated Equipment Group Dallas, Texas 75222		10. PROGRAM ELEMENT, PROJECT, TASK AREA & WORK UNIT NUMBERS VELA T/2705/B/ASD
11. CONTROLLING OFFICE NAME AND ADDRESS Advanced Research Projects Agency Nuclear Monitoring Research Office Arlington, Virginia 22209		12. REPORT DATE 30 November 1973
		13. NUMBER OF PAGES ~~34~~ 36
14. MONITORING AGENCY NAME & ADDRESS(if different from Controlling Office) Air Force Technical Applications Center VELA Seismological Center Alexandria, Virginia 22314		15. SECURITY CLASS. (of this report) UNCLASSIFIED
		15a. DECLASSIFICATION/DOWNGRADING SCHEDULE

16. DISTRIBUTION STATEMENT (of this Report)

APPROVED FOR PUBLIC RELEASE, DISTRIBUTION UNLIMITED

17. DISTRIBUTION STATEMENT (of the abstract entered in Block 20, if different from Report)

18. SUPPLEMENTARY NOTES

ARPA Order No. 1714

19. KEY WORDS (Continue on reverse side if necessary and identify by block number)

Adaptive Filter
Surface Waves
Particle Motion

20. ABSTRACT (Continue on reverse side if necessary and identify by block number)

The three-component adaptive filter takes advantage of the phase relations between radial, vertical, and tangential seismometer traces which hold when Rayleigh and Love waves are present. This study finds that adaptively processed data has up to 6 dB greater signal-to-noise ratio than simple bandpassed data. The detection threshold for single site data is lowered by an amount consistent with this gain, but the detection threshold for beam data is unchanged. An explanation for this difference, based on

DD FORM 1473 1 JAN 73   EDITION OF 1 NOV 65 IS OBSOLETE

20. continued

the character of single site and beam noise fields, is presented.
Azimuthal discrimination and response of the filter to random
noise are investigated.

ALEX(01)-STR-73-15

EVALUATION OF AN ADAPTIVE THREE-COMPONENT FILTER

SPECIAL REPORT NO. 15

EXTENDED ARRAY EVALUATION PROGRAM

Prepared by
Stephen S. Lane

TEXAS INSTRUMENTS INCORPORATED
Equipment Group
Post Office Box 6015
Dallas, Texas 75222

Prepared for

AIR FORCE TECHNICAL APPLICATIONS CENTER
AFTAC Project No. VELA T/2705/B/ASD
Alexandria, Virginia 22314

Sponsored by

ADVANCED RESEARCH PROJECTS AGENCY
Nuclear Monitoring Research Office
ARPA Program Code No. 2F10
ARPA Order No. 1714

30 November 1973

Equipment Group

ABSTRACT

A three-component adaptive filter has been developed at Lamont-Doherty Geological Observatory. It takes advantage of the phase relations between radial, vertical, and tangential seismometer traces which hold when Rayleigh and Love waves are present. This study finds that adaptively processed data has up to 6 dB greater signal-to-noise ratio than simple bandpassed data. The detection threshold for single site data is lowered by an amount consistent with this gain, but the detection threshold for beam data is unchanged. An explanation for this difference, based on the character of single site and beam noise fields, is presented. Azimuthal discrimination and response of the filter to random noise are investigated.

TABLE OF CONTENTS

iv

LIST OF FIGURES

LIST OF TABLES

vi

SECTION I
INTRODUCTION

The adaptive filter studied here was developed at the Lamont Geophysical Observatory (Shimshoni and Smith, 1964) and is a three component processor designed to improve the detectability of long-period Rayleigh and Love waves. It takes advantage of the fact that when Rayleigh and Love waves are present there is a known phase relationship on the three mutually perpendicular long-period seismometer traces. Potentially, improvements in signal-to-noise ratio can be achieved when these phase relationships are utilized in the processor design.

This report presents results of an evaluation of the adaptive filter using both synthetic and real data. Synthetic data included known signals buried in noise at various signal-to-noise ratios, used to study the filters signal-to-noise improvement characteristics; and random noise used to study the processors false alarm characteristics. Real data included single site and beam data from the Alaskan Long Period Array (ALPA) and single stations from the Very Long Period Experiment (VLPE) network (Lambert, 1973), used to study the processors detection performance.

SECTION II
DESCRIPTION OF THE ADAPTIVE FILTER

This adaptive filter (Shimshoni and Smith, 1964) forms a
three component filter in the frequency domain which passes energy having
the characteristics of Love and Rayleigh waves. The filter is adaptive, be-
cause the data are segmented and a new filter designed for each segment.
The filter weights depend on the signal behavior during the segment, rather
than the behavior for some fixed time before or after the output point.

To pass Rayleigh waves, the processor looks for signals which
are 90° out of phase on the radial and vertical components. The Fourier
transform of a segment of data is taken, and the phase angle between radial
and vertical components calculated at each frequency. This angle will be
$\pi/2$ for pure Rayleigh waves. Some power of the sine of this angle constitutes
the frequency domain filter weight for the frequency in question, for the seg-
ment being processed.

Relevant equations for the design of the Rayleigh wave filter
are given below. Suppose that the vertical and radial time traces for the n-th
segment of data are given by V_n and R_n. Then at the i-th frequency the
Fourier transforms for those segments are $\widetilde{V}_n(i)$ and $\widetilde{R}_n(i)$. These com-
ponents are complex numbers and may be written as:

$$\widetilde{V}_n = \left| \widetilde{V}_n(i) \right| e^{j\phi_n(i)} \qquad \widetilde{R}_n = \left| \widetilde{R}_n(i) \right| e^{j\psi_n(i)}$$

The phase angle between the vertical and radial is then

$$\phi_n(i) - \psi_n(i)$$

and the filter weight is

$$F_n(i) = \sin^N(\varphi_n - \psi_n) \qquad \text{where N must be an even integer}$$

An $F_n(i)$ is calculated for every frequency, and the new Fourier series $\widetilde{r}_n(i)$ and $\widetilde{v}_n(i)$ are formed.

$$\widetilde{v}_n(i) = F_n(i) \, \widetilde{V}_n(i) \qquad \widetilde{r}_n(i) = F_n(i) \, \widetilde{R}_n(i) \quad .$$

The inverse transforms of these series are the filtered time traces for the n-th segment.

The n+1 segment of time data is taken beginning at the mid-point of the n-th segment. After filtering as above, a weighted average of the segments is formed over their common interval, with weights which sum to 1 and which are proportional to the time from the end point of the interval. Thus discontinuities in the time output are avoided.

Figure II-1 gives a graphical representation of the determination of a filter weight for Rayleigh motion. Here at a single frequency the transforms of the vertical and radial motion are plotted in polar form, and are seen to be composed of a signal and noise contribution. The phase of the radial signal has arbitrarily been chosen to be zero. The phase of the vertical signal is therefore $\pi/2$. The phases of the noise contributions are random. The net phase difference between the radial and vertical components is θ , and the filter weight designed for this frequency is $\sin^N \theta$.

When the amplitude of the noise components is much less than that of the signal components θ will be nearly $\pi/2$, and the filter weight will be large. If the noise is large and random, the weight will be small, and little of the energy present will be passed. Here the adaptive filter differs markedly from the bandpass filter; the bandpass filter will pass all energy, due to signal or noise, within its frequency range. The adaptive filter discriminates against frequencies where there is more noise than signal.
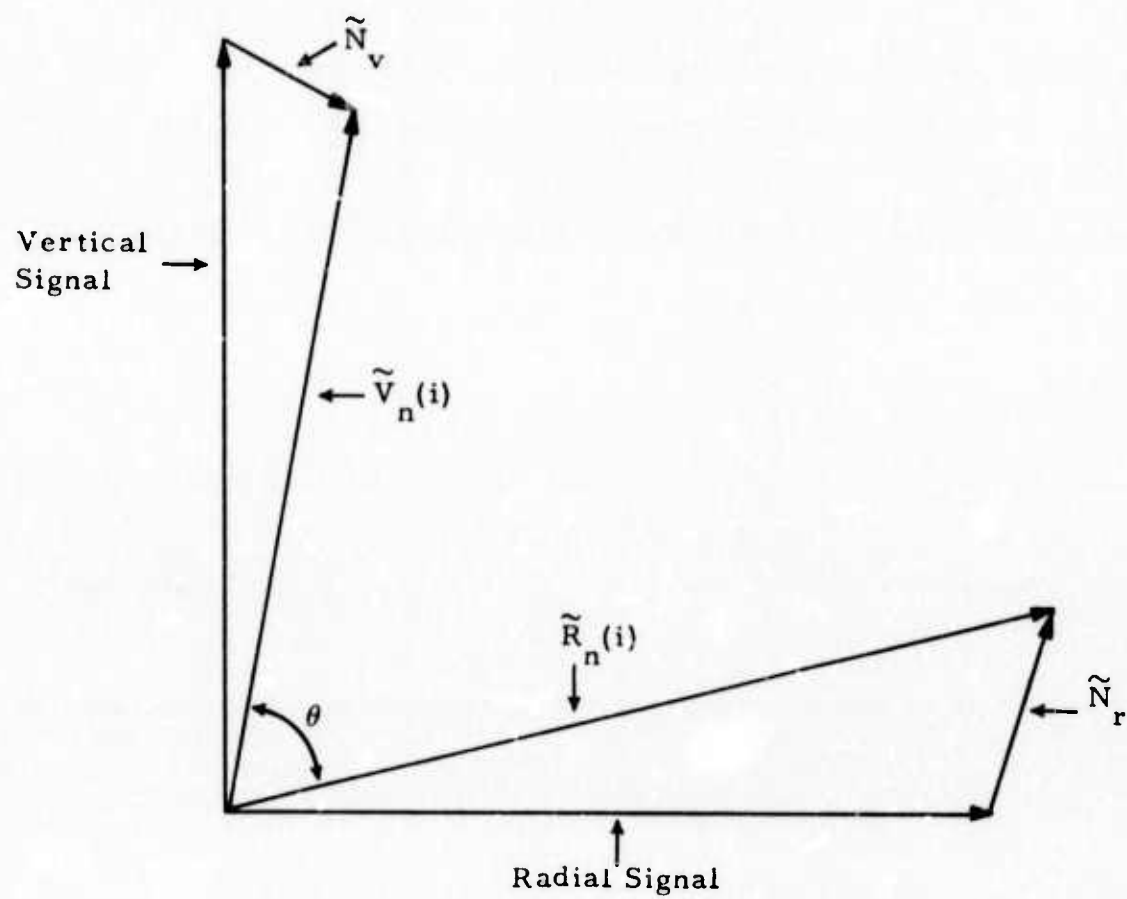
II-2

FIGURE II-1

FOURIER COMPONENTS FOR RAYLEIGH WAVE FILTER DESIGN

There is no such phase relation for the Love wave as there is for the Rayleigh wave, because the Love wave, when properly oriented, appears only on the transverse component. This fact is used to design the Love wave filter as shown in Figure 11-2. This is a plot of the amplitudes of particle motion in the radial and transverse directions independent of their phase angles, rather than a polar plot of complex numbers. Along the transverse and radial directions the magnitude of the transverse and radial Fourier components at the frequency in question are plotted. The angle $\alpha(i)$ is used to design the filter weight through

$$G(i) = \cos^N(\alpha(i))$$

This filter weight is applied to the transverse component only. The exponent here is the same as that for the Rayleigh filter. An off-azimuth Love wave will be discriminated against, since a portion of its amplitude will appear on the radial trace. Any motion on the radial trace will reduce the Love wave amplitude, in fact. In particular, the Rayleigh wave is interpreted by the filter as an off-azimuth Love wave, and that portion of the Love wave which occurs at the same time as the Rayleigh wave is suppressed.

A few comments may be made about the parameters in the filter before the results are discussed. The rate of adaption is important, and decreases as the segment length increases. Other things being equal, a high adaption rate would be desirable, but as segment length decreases, window effects produce distortion in the output trace. Segments of 128 seconds worked well for the 17-42 second data processed here.

It might seem reasonable to process the output traces again with the adaptive filter to discriminate further against noise. Examination of the equations will show that this corresponds to doubling the exponent of the trigonometric functions in the filter design.

11-4

FIGURE II-2

FOURIER COMPONENTS FOR LOVE WAVE FILTER DESIGN

Increasing the exponent of the trigonometric functions narrows the range of phase and spatial angles over which energy can be passed. Because signals will always be contaminated with noise, the radial-vertical phase angle will never be just 90°, nor the Love polarization angle just 0°. These angles will rather occupy some range about their ideal values. If the exponents are made too large, significant amounts of signal energy will be rejected along with the noise. Thus there is an optimum value for the exponents of the trigonometric functions, and this value seems to be six for our data.

The adaptive filter can be applied to both beamed and single site data. A third possibility is to apply the processor to a number of individual sites and form a beam from the results.

SECTION III

RESULTS

The following kinds of records were processed to evaluate the adaptive filter:

- Single-site ALPA signals were buried in noise, and the gain in signal-to-noise ratio produced by the adaptive filter found as a function of the original signal-to-noise ratio.

- ALPA beam data were buried in noise and processed as above.

- A number of ALPA beam records were processed as recorded and the signal-to-noise ratio improvement and detection probability improvement found.

- VLPE records were processed as above.

- The adaptive filter was applied to synthetic data output from a random number generator.

- Angular resolution studies were made on single station ALPA records.

Some general remarks may be made about the results. First, radial and vertical traces followed the same sort of behavior. As the signal emerged from the noise, the gain in signal to noise ratio of the processed over bandpassed-only signals increased to about 5-8 dB. From this point further increases in signal-to-noise ratio did not increase the filter's gain, and at large enough signals, the gain actually dropped back toward zero.

Behavior of the Love wave is more erratic, because, as mentioned above, it is suppressed by the presence of the Rayleigh wave. No large gains on the transverse component were found; a loss of signal-to-noise ratio was common. The specific behavior depended on the time separation between Love and Rayleigh wave onsets. Larger time separations gave rise to larger gains.

The above conclusions apply to both single-site and beamed data. However, detection probability was not affected in the same way for the two kinds of data. The detection rate was essentially unchanged for adaptively processed beam data, but increased by a factor of about two for single site data. The difference is due to the relatively greater importance of propagating noise on the beam data, and will be discussed later.

A. SINGLE STATION PROCESSOR GAINS

Two summer and two winter events recorded at ALPA during 1972 were selected for processing. Motion over a 4096 second segment containing a large ("noise-free") signal recorded at site 1 was, for each event, multiplied by a scale factor and added to the noise in a 4096 second segment preceding the signal segment. The adaptive filter was applied to the resulting composite trace. The data were also subjected to a bandpass filter which rejected all energy outside the .024 - .059 Hz (17 to 42 second) band. A wide range of scale factors was used for each event, so that the raw traces ranged from the case where the signal was completely buried in noise to where it was clearly visible.

Output signal-to-noise ratios were calculated by dividing the peak value of the processed trace, within the arrival time window, by the root mean square value of the noise in the composite trace over the time prior to the signal arrival time. Twenty times the log of this quantity is the signal-to-noise ratio. Noise to noise ratios were found by dividing the peak of the noise trace by the root mean square value of the noise.

Signal-to-noise ratios were calculated for both adaptively processed and bandpassed traces. The gain of the adaptive filter over the bandpass filter is the difference between the signal-to-noise ratios of the adaptive filter and the bandpass filter for the same event.

There was a great deal of variation in the details of behavior from event to event. In Figure III-1 results for a fairly typical event, KAM-199-08AL, are plotted. The horizontal axis is the true signal-to-noise ratio, in dB, of the composite trace before processing. This value was obtained by multiplying the peak value of the noise free signal, before scaling, by the scale factor, and dividing by the RMS value of the unprocessed noise. Twenty times the logarithm of this quantity is the true signal-to-noise ratio. The vertical axis is the gain of the adaptively processed trace over the bandpassed trace, at the same scale factor.

The vertical and radial components follow the same general trend. They have roughly constant gains of 3 dB below about 0 dB signal-to-noise ratio. Below about -5 dB, where the signal was detected, the peak amplitude was not due to the signal but to a propagating noise arrival. If this noise peak had not been present the gain would have dropped below 3 dB. Above 0 dB the adaptive filter shows even more gain over the bandpass filter. The gain in general reaches about 6 dB and then drops toward zero as all the filter weights approach one.

The transverse component for this event was considerably larger than the radial and vertical components. Therefore, the Rayleigh wave is not interpreted as an off-azimuth Love wave, and the transverse component shows gain down to low signal-to-noise ratios. The same increase in gain near zero dB is present as on vertical and radial traces.

Figure III-2 shows a composite raw signal, the same signal after bandpass filtering, and after application of the adaptive filter. In this case the signal is clearly visible only on the adaptive filter output.
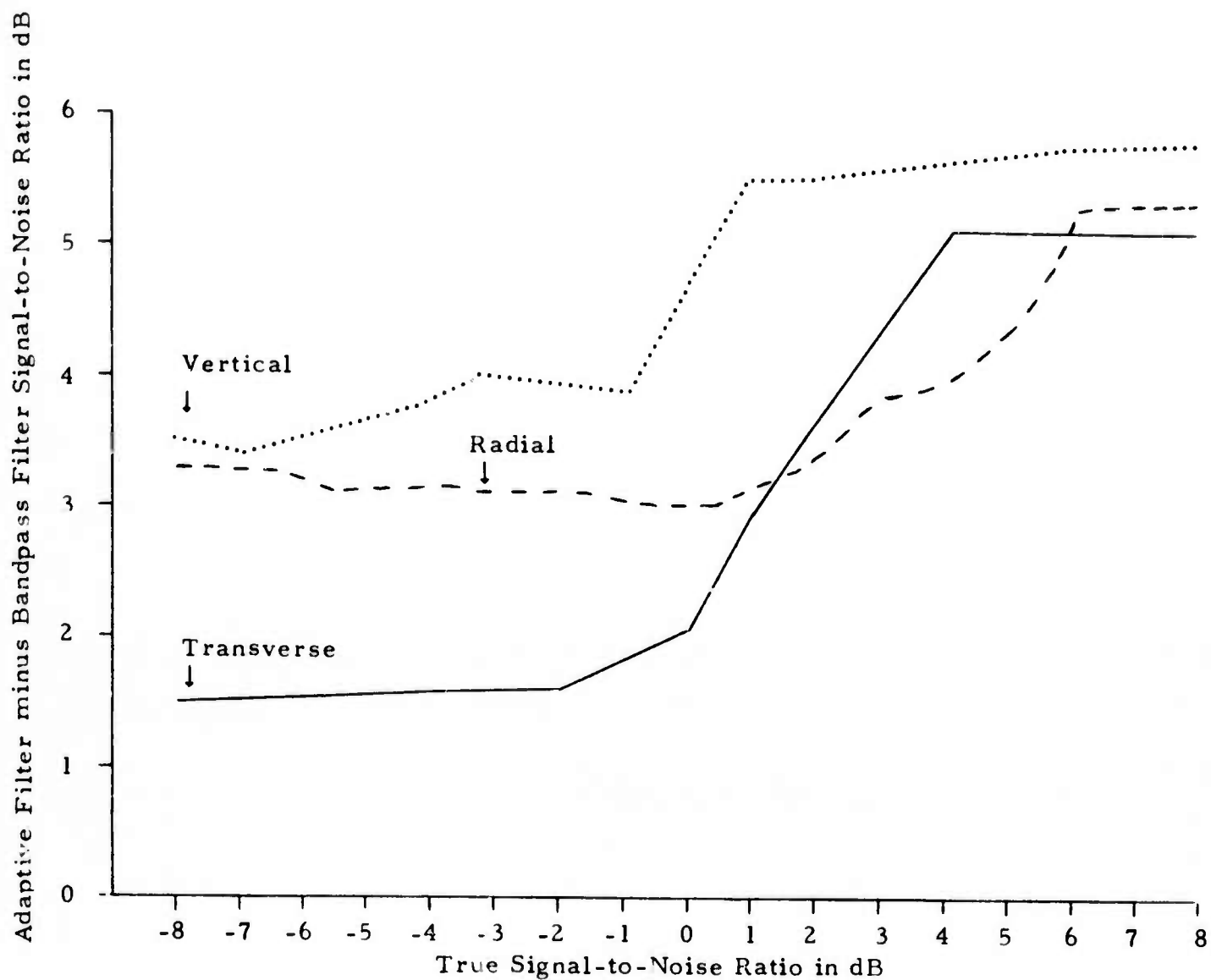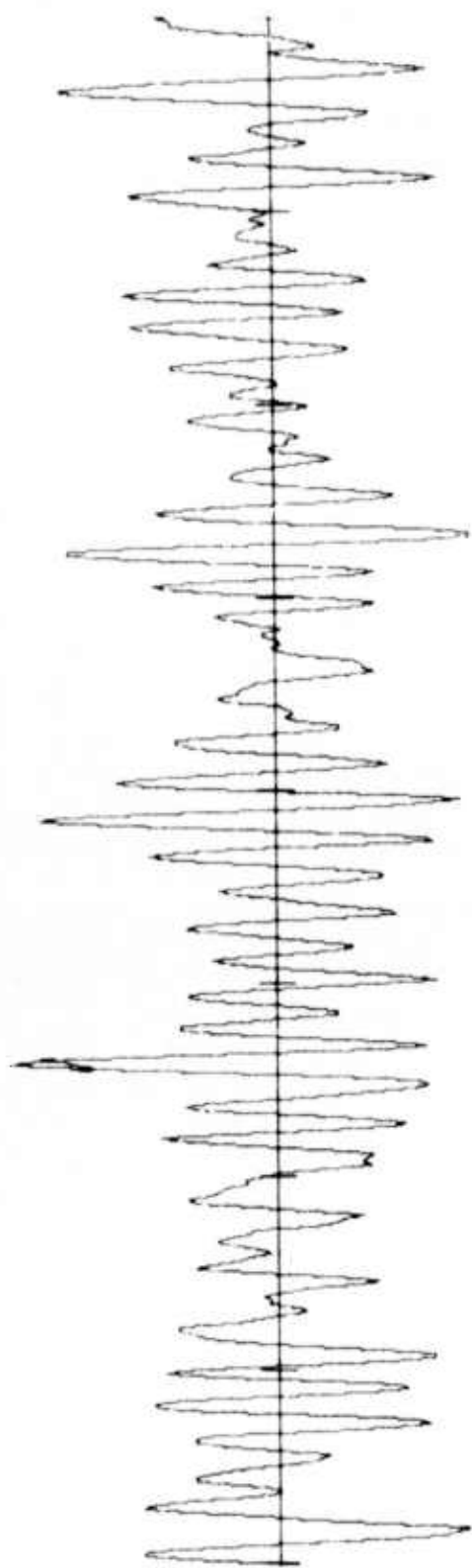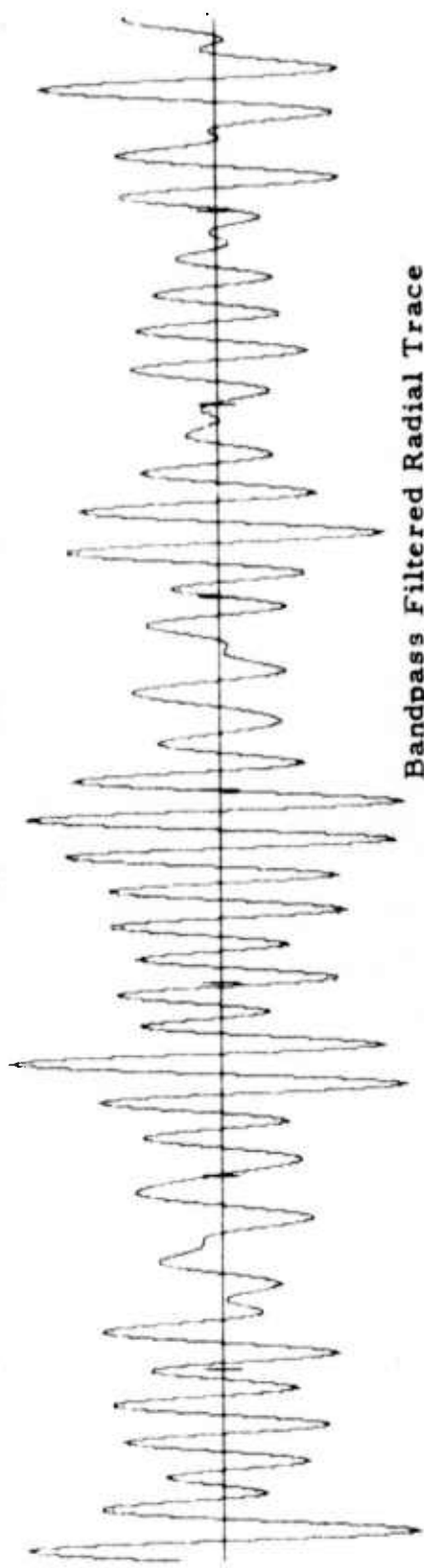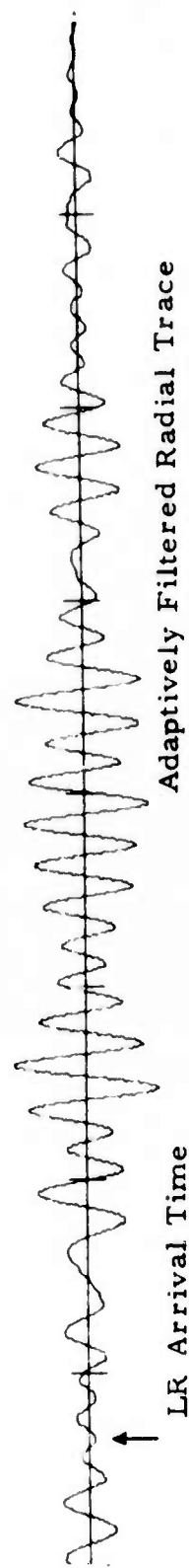
III-3

FIGURE III-1

GAIN VERSUS SIGNAL-TO-NOISE RATIO FOR SINGLE SITE DATA

Composite Radial Trace

Bandpass Filtered Radial Trace

Adaptively Filtered Radial Trace

LR Arrival Time

FIGURE III-2

TIME TRACES FOR SINGLE STATION RADIAL DATA

III-5

B. BEAM PROCESSOR GAINS

To find the filter's gain on beam data, 2048 seconds of data in the signal gate were added with a scale factor to the 2048 seconds of noise data immediately preceding them. The scale factor was varied as before, and the gain of the processed trace's signal-to-noise ratio over that of bandpassed data was plotted versus true signal-to-noise ratio. The results again for event KAM-199-08AL are shown in Figure III-3. For this beam record there was no noise peak in the signal gate. At a true signal-to-noise ratio of about 1 - 4 dB the adaptive filter starts to show gain with respect to the bandpassed data. This gain reaches a maximum of about 6 - 8 dB for the radial and vertical motion, and the transverse gain is constant. Thus the adaptive filter requires larger signal-to-noise ratios on beam data than on single site data before gain and detection take place.

This difference in the point at which the filter starts to show gain is significant in terms of detection probabilities. In general, the adaptive filter shows gain for beam data only for signals which were detected anyway, but applied to single station data it lowers the detection threshold. In this case the threshold was lowered about 6 dB. Criteria used here for determining detections are presented by Strauss (1973).

An explanation for this effect may be found by examining the character of the noise field in the different kinds of records. On single site records the noise is a mixture of non-propagating noise and propagating Love and Rayleigh waves from various azimuths. The radial component, for example, then contains contributions from Love waves and Rayleigh waves. These waves are added with various weights ranging from -1 to +1, depending on the azimuth of the noise source. As a result there is no special phase relationship between the vertical and radial Fourier coefficients at any given frequency.
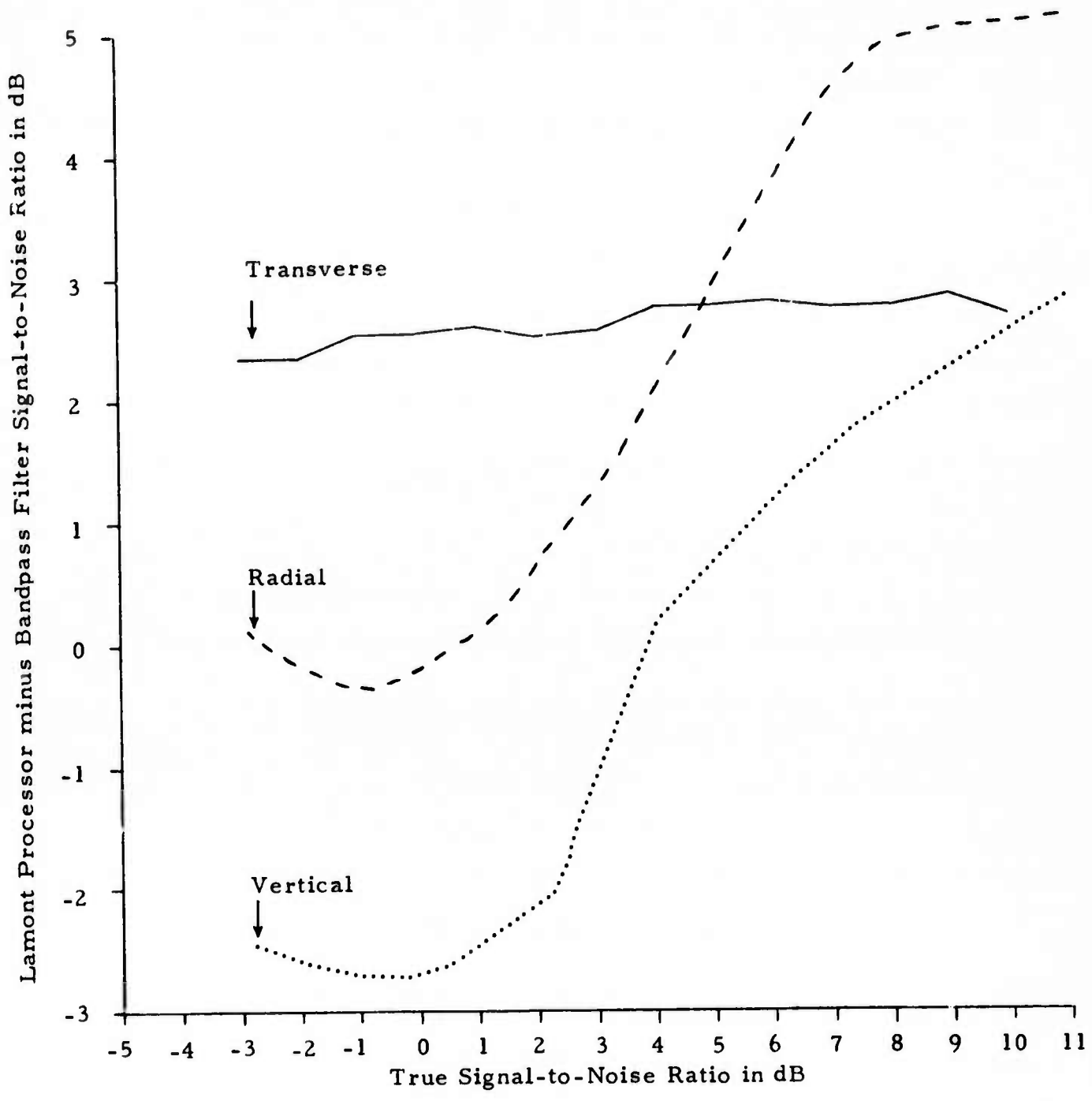
FIGURE III-3

GAIN VERSUS SIGNAL-TO-NOISE RATIO FOR BEAM DATA

The filter therefore calculates a low filter weight for this kind of noise. That is, the adaptive filter responds to propagating noise from various directions, at a single site, as though it were random noise. When a signal is encountered the filter weights change towards one, as they should. The result is an improvement in signal-to-noise ratio.

On beam records the process of beamforming has greatly reduced the propagating noise, except for that which comes from the signal azimuth, which suffers relatively little attenuation. Random noise is also greatly reduced, so the resulting motion contains a large fraction of Love and Rayleigh waves coming from the signal direction.

This propagating noise has the correct phase relationship to be passed by the filter. Consequently filter weights are high and this noise is not suppressed. Now when a signal arrives it is effectively being added to another signal, not to noise. Consequently there is little change in the filter weights, and there is no improvement in signal-to-noise ratio.

To test this hypothesis the noise sample preceding event KAM-199-08AL was investigated. The RMS noise amplitudes, at a single site, were calculated with both bandpass filter and adaptive filter. The change in amplitude is a measure of noise reduction by adaptive filter processing single site data. This noise reduction averaged 9.3 dB for all components.

The same experiment was performed for the same noise samples using the full array. The beam was not aimed at any large noise source. Reduction in this case averaged 6.8 dB, 2.5 dB less than in the single site case. This improved suppression of single site noise tends to confirm the explanation given for superior performance on single site data.

The question then arises as to why any improvement at all is achieved on beam records. When the true signal is added at high enough level, filter weights are indeed changed toward one. More signal is required to achieve a change, for the reasons given above.

C.   BEAM RECORDS

Twenty-three events, listed in Table III-1 were recorded at ALPA and beams formed. These signals were processed with the adaptive filter and by bandpassing. Figure III-4 shows these events plotted in a way analogous to Figures III-1 and III-3. The horizontal axis is magnitude, and the vertical axis is the gain of the adaptive filter over bandpassing. Only radial components are plotted. The behavior of the other two components was similar.

Magnitude and detection status are also listed in Table III-1. Two events were detected by the adaptive filter but not by the bandpass filter. However, three events not detected by the adaptive filter were at least marginally detected by the bandpass processor. In all other cases there was no change in status when events were processed one way of the other.

The behavior of the points of Figure III-4 is much more erratic than that of Figure III-3, because many different events were used. The general trend shows an increasing number of detections and increasing gain of the adaptive filter over the bandpass filter as the magnitude increases. Eventually there is a reduction in gain.

It might be thought that a change in detection threshold could be achieved by processing each site with the adaptive filter, and then forming a beam. This is not the case for the following reason. Filter weights for the adaptive filter are always less than one, so there is always signal degradation. The degradation is less when the signal-to-noise ratio is high, as after beamforming. Beamforming, in the ideal case, results in no signal degradation. Thus the signal is reduced overall by adaptive filter processing before beamforming compared to processing in the reverse order.

III-9

TABLE III-1

ADAPTIVELY PROCESSED BEAMS (VERTICAL COMPONENT)

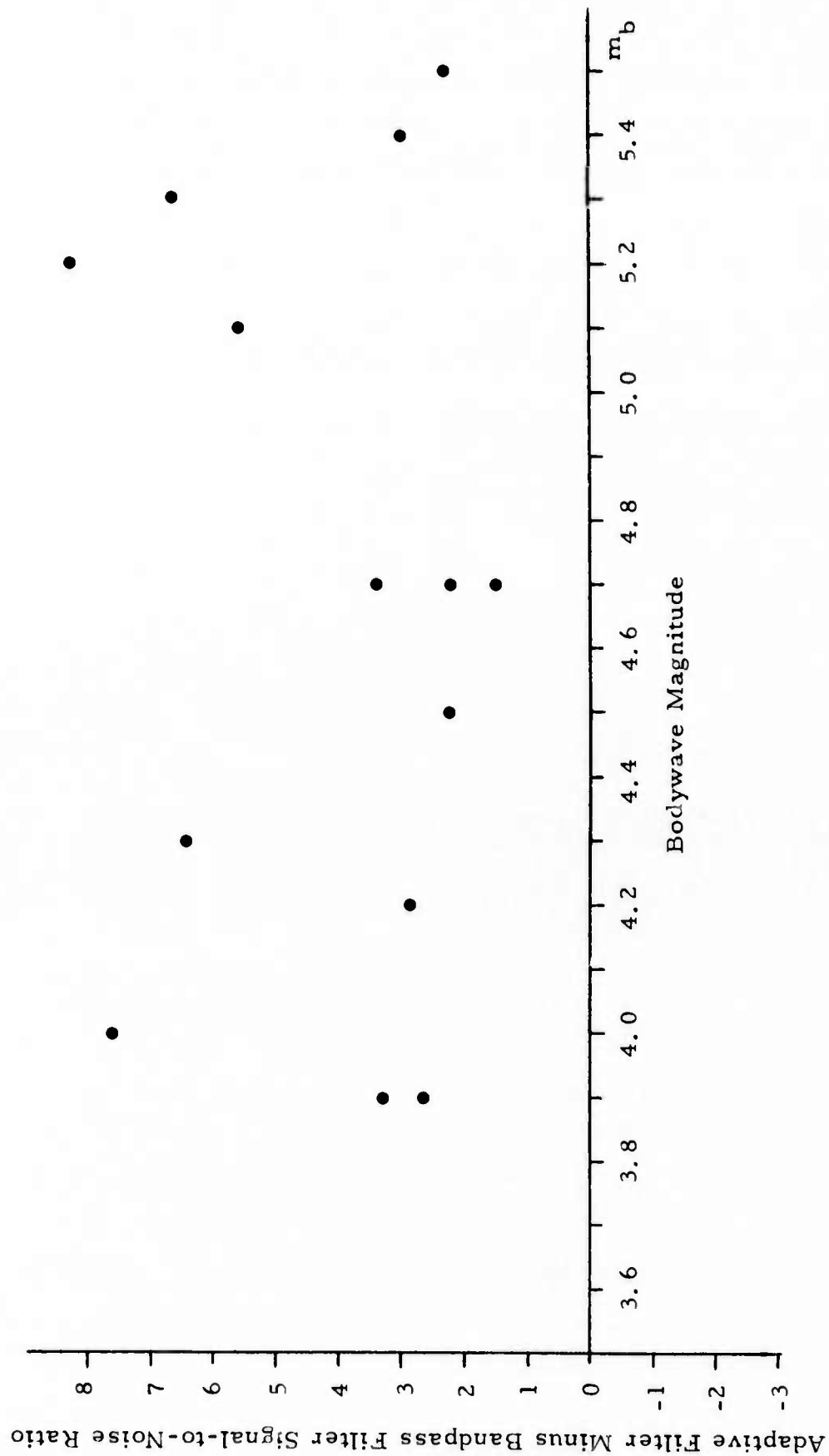| Region	Event	m_b	Adaptive Filter	Bandpass Filter
Kurile Islands	KUR-162-19AL	3.7	N	N
	KUR-195-15AL	4.2	D	D
	KUR-197-09AL	4.4	N	D
	KUR-197-17AL	3.5	N	N
	KUR-216-02QC	4.5	D	D
	KUR-217-04AL	4.0	D	N
	KUR-228-22AL	4.1	N	N
	KUR-232-21AL	3.5	N	Marg. D
	KUR-234-13AL	4.0	N	N
	KUR-235-03AL	4.1	N	Marg. D
Iran-Iraq	IIQ-157-11AL	3.9	D	N
	IIQ-162-19AL	4.0	D	N
	IIQ-164-13AL	5.4	D	D
	IIQ-165-00AL	5.1	D	D
	IIQ-166-04AL	5.3	D	D
	IIQ-185-19AL	4.0	N	N
	IIQ-193-22AL	4.7	D	D
Tibet	TIB-170-04AL	4.3	D	D
	TIB-195-05AL	3.9	N	N
	TIB-198-02AL	5.2	D	D
	TIB-198-03AL	4.7	D	D
	TIB-204-16AL	5.5	D	D
	TIB-204-21AL	4.7	D	D

D = Detected

N = Not Detected

FIGURE III-4

GAIN VERSUS BODYWAVE MAGNITUDE FOR BEAMS

Noise is reduced as well, according to the above arguements, so experimental verification was required. Three events were processed in one order and then the other. In two of the nine traces, adaptive filter processing before beamforming showed a gain in signal-to-noise ratio. In the other seven cases adaptive filter processing before beamforming was inferior. The average loss using this order of processing was 2.3 dB.

The agreement between Figures III-3 and III-4, the insignificant change in number of detections, and the arguements of this section lead to the conclusion that the adaptive filter is of little value when applied to beam data.

D.   VLPE DATA

There is little practical value in applying the adaptive filter to single stations which are part of an array, since beamforming will yield about 10 dB improvement, and it has been shown that there is no gain in adaptive filter processing before beamforming rather than after. A better candidate is the VLPE network of single stations as described by Lambert et. al., (1973). These stations can be expected to behave as do single array stations with respect to signal-to-noise improvements. Therefore a suite of events, as recorded, was processed with the adaptive filter and with simple bandpass filtering, and the detection probability determined.

The events processed are discribed in Table III-2 using Lambert's notation. Sixty-nine records from 22 events, ranging in bodywave magnitude from 3.2 to 4.8 were processed. The number of detections at a given magnitude, expressed as a percent of the number of possible detections, is plotted against bodywave magnitude in Figure III-5, for bandpassed and adaptively processed data. A histogram of the number of possible detections at each magnitude is also presented.

TABLE III-2

VLPE EVENTS PROCESSED

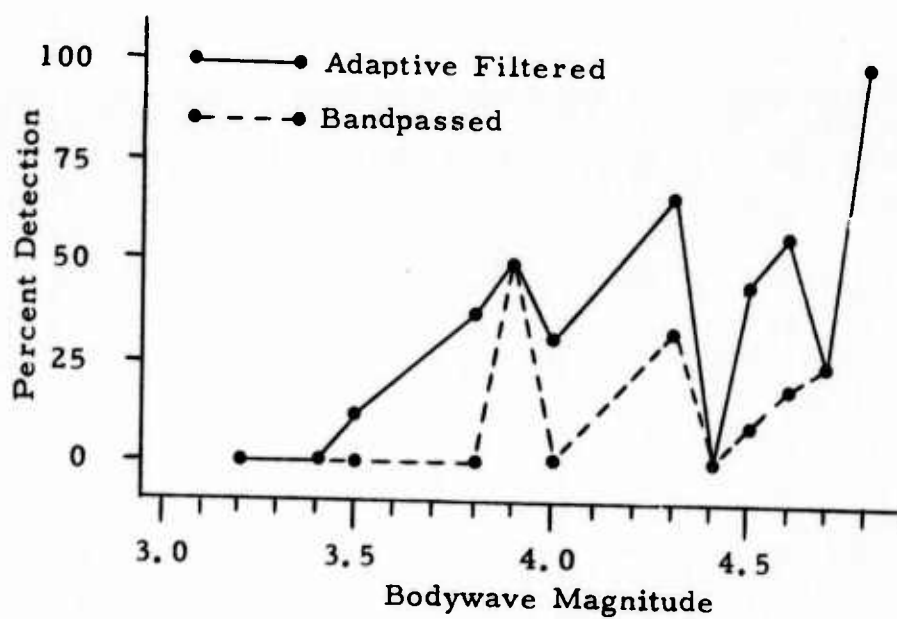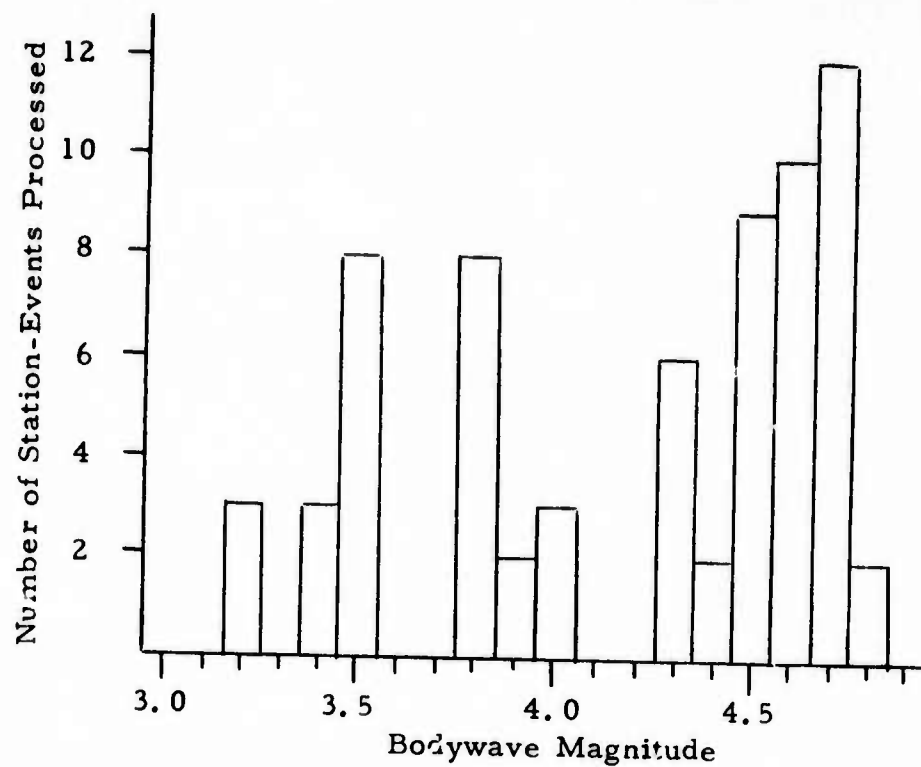| Event Number	Month	Day	Origin Time	m_b	Lat °N	Long °E
0021	01	06	06.30.36	4.7	40.7	72.4
0045	01	15	20.45.22	4.6	39.3	79.9
0075	01	28	20.29.09	4.5	40.8	81.4
0108	02	06	07.30.11	4.7	41.6	82.2
0129	02	16	23.19.20	4.8	41.7	80.7
0225	03	02	19.57.42	3.5	43.0	76.0
0235	03	04	04.00.09	4.5	40.0	80.0
0236	03	04	08.22.16	4.4	43.0	86.0
0302	03	18	19.54.18	3.2	41.0	72.0
0309	03	20	21.47.55	3.4	40.0	80.0
0317	06	02	04.21.49	3.8	42.0	82.0
0319	06	02	05.11.13	3.5	43.0	81.0
0320	06	02	06.30.49	3.9	42.0	81.0
0384	06	18	09.18.49	4.3	40.0	73.0
0449	07	05	01.09.53	4.6	44.6	81.1
0450	07	05	02.41.54	3.5	44.0	86.0
0451	07	05	04.09.49	4.3	43.6	87.9
0470	07	10	19.03.33	4.7	43.4	88.6
0491	07	15	00.35.52	3.8	43.0	78.0
0510	07	18	03.27.07	4.0	39.0	77.0
0536	07	28	05.50.29	4.3	42.0	81.0
0604	08	09	16.28.14	4.5	41.0	72.0
0662	08	22	16.34.56	4.6	40.0	79.0

FIGURE III-5

PERCENT DETECTION VERSUS m_b FOR VLPE DATA

III-14

Nowhere does the adaptive filter have a lower detection pro-
bability than the bandpass filter, and in general its detection probability is
higher. Out of the total sample, the adaptive filter detected 37% and the
bandpass filter 11% of the events.

An improvement in signal-to-noise ratio of 6 dB, as found
in section A, implies a reduction of about 0.3 in the magnitude where 50% of
all events are detected, and consequently a doubling of the total number of
events detected. Our data sample is too small to accurately determine the
50% detection level, but the tripling of total detection probability is not in-
consistent with the measured increase in signal-to-noise ratio.

E.   RANDOM NOISE SAMPLE

About 12-thousand seconds of random Gaussian three-component
noise, with mean zero and standard deviation unity, was generated and
filtered with the adaptive filter and the bandpass filter. Typical output
time traces are shown in Figure III-6. The radial and vertical traces show
nothing that looks like a Rayleigh wave. When the radial motion, by chance,
is small, the transverse motion is passed, and is larger than usual. How-
ever, these cycles do not appear "signal-like" (i.e., they show no dispersion
and do not persist in time). We therefore conclude that the contribution of
random noise to the false alarm rate for the adaptive filter is essentially zero.

The response of the filter to recorded noise is as shown in
the first part of Figure III-2. What look like small signals appear on all three
traces. Presumably they are due to a larger burst of propagating noise than
usual. Since all filter weights are less than one we know that there was indeed
motion on those axies of at least the magnitude shown. Thus any peaks on
the filter output are due to propagating noise within the signal gate. Lack
of dispersion precludes the confusion of these peaks with true seismic events.

Adaptive Vertical

Adaptive Transverse

Adaptive Radial

100 sec.

FIGURE III-6

RESPONSE TO RANDOM NOISE

III-16

F.   AZIMUTHAL DISCRIMINATION

An event recorded at a single ALPA site with good signal-to-noise ratio was processed with the seismometer axies rotated various amounts from the primary beam direction.   The peak amplitude of the various components was recorded, normalized to unity at its maximum value, and plotted as a function of azimuth from the primary beam direction.   The results are shown in Figure III-7.

Apparently the event chosen is slightly multipathed because the peak motion on the transverse and radial axies comes about 15 degrees from the expected one.   The amplitude falls off rather slowly with angle for the vertical and radial axies, due to the increased projection of the Love motion on the radial axis and consequent contamination of the phase difference between vertical and radial components.   Since the same filter weight is applied to vertical as radial, the vertical motion is also attenuated with misalignment.

The transverse resolution is much higher, since the filter specifically rejects off-azimuth motion.   The transverse half width at half power is about 15 degrees.
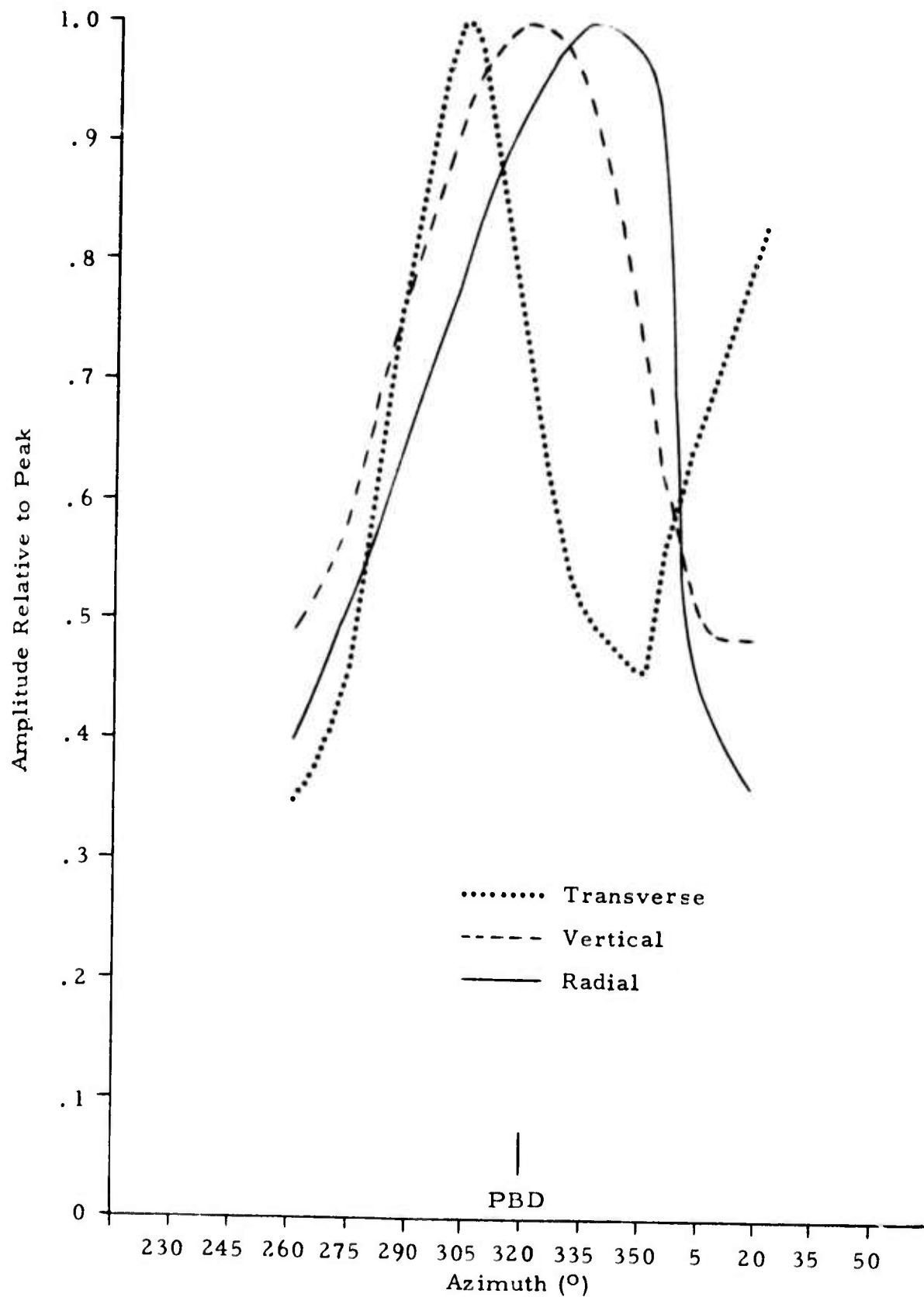
FIGURE III-7

AZIMUTHAL RESPONSE

III-18

SECTION IV
CONCLUSIONS

The following conclusions are based on a comparison of the performance of the adaptive filter with a simple bandpass filter on single site and beam data from ALPA, data from the VLPE network, and on synthetic data.

The adaptive filter output can have as much as 8 dB improvement in signal-to-noise ratio over the bandpass filter output, for both single site and beam data. However, gain is achieved on beam records only when signals are already detected on bandpass filter outputs. Thus no gain in detections results from application to the processor to beam data. This behavior can be understood from an analysis of the noise present there. No improvement was found when the adaptive filter was applied before beam-forming rather than after.

Gain in signal-to-noise ratio on single site data takes place even when the signal was not detected on bandpassed records. Thus an increase in detections is possible. For the sample of events reported, recorded at the VLPE stations, the percent of detections rose from 11% to 37% when the adaptive filter replaced the bandpass filter. The percent of detections at each magnitude was as large as, or larger, when the adaptive filter was used than when only bandpass filtering was used.

The adaptive filter did not reduce the amplitude of mis-oriented Rayleigh waves much more than the geometrical factor to be expected from incorrect alignment of the axies. However, the Love wave rejection of off-azimuth signals was much greater than that expected from misalignment alone.

The adaptive filter does not create spurious signals from noise. Its false alarm rate thus depends on the analysts ability to distinguish propagating noise from seismic signals.

For these reasons it is recommended that the adaptive filter be routinely used to process VLPE data, but that it not be used on beam data.

SECTION V
REFERENCES

Lambert, D. G., and E. S. Becker, 1973, Evaluation of the Detection and Discrimination Capabilities of the Very Long Period (VLPE) single Stations, VLPE Network, and the VLPE-ALPA-NORSAR Combined Network, Special Report No. 6, Texas Instruments Incorporated.

Shimshoni, M., and S. W. Smith, 1964, Seismic Signal Enhancement with Three-Component Detectors, Geophysics, 29, p. 664.

Strauss, A., 1973, Final Evaluation of the Detection and Discrimination Capability of the Alaskan Long Period Array, Special Report No. 8, Texas Instruments Incorporated.